Elastic moduli of tungsten to 15 Mbar, phase transition at 6.5 Mbar, and rheology to 6 Mbar

Arthur L. Ruoff
Department of Materials Science and Engineering, Cornell University, Ithaca, New York 14853

C. O. Rodriguez
Instutito de Fisica de Liquidos y Sistema Bilogica, Grupo de Fisica del Solido, C.C. 565, La Plata, Argentina

Niels E. Christensen
Institute of Physics and Astronomy, Aarhus University DK-8000, Aarhus, Denmark
(Received 11 March 1998)

The elastic constants of the bcc and fcc structures of W at 0 K versus reduced volume and pressure were obtained from first-principles, all-electron, density-functional calculations to $V/V_0=0.40$ ($P=15.3$ Mbar). The dhcp and the fcc phase were calculated to be more stable than the bcc phase above 6.5 Mbar. The energy versus c/a along Bain's path was calculated for different fractional volumes. The single-crystal constants of the bcc structure were used to calculate the shear modulus G of the polycrystalline bcc aggregate versus pressure. These results were used with the Chua and Ruoff pressure scaling relation to show that at 6 Mbar, the yield strength has increased by a factor of 4.5. The pressure dependence of the yield strength is compared with recent measurements. [S0163-1829(98)02930-0]

I. INTRODUCTION

Of the metallic elements at atmospheric pressure, W and Re have the largest bulk and shear moduli. The large values of the shear moduli help explain the high compressive strength of these metals. Both materials have been used for gaskets in diamond-anvil cells for this reason.[1,2] The substantial increase in the shear moduli at ultrahigh pressures increases the strength (pressure strengthening) and makes it possible to contain pressures greater than that at the earth's core using gaskets of these materials.[3] The high strength of W has made it possible to achieve pressures above 3 Mbar on hydrogen in attempts to metallize it.[4]

For many solids, there have been extensive calculations of the bulk modulus over a large pressure range.[5] There have been fewer calculations of the complete set of elastic constants over a wide pressure range, although some studies have been made.[6,7] In the present case, a detailed study was made of the elastic moduli of W for both the bcc phase (which is calculated to be the equilibrium structure to 6.5 Mbar) and the fcc phase to a volume fraction $V/V_0=0.40$. The results for the shear constants $C'=(C_{11}-C_{12})/2$, C_{44} and the bulk modulus B of the bcc phase are used with the variational method of Hashin and Shtrikman[8] to compute the shear modulus $G(P)$ and the Poisson ratio $\nu(P)$ of the randomly oriented polycrystalline aggregate. From these and the Chua and Ruoff scaling law,[9] the pressure dependence of the yield strength $\sigma_0(P)$ was obtained.

II. CALCULATION OF SINGLE-CRYSTAL ELASTIC CONSTANTS

The elastic shear constants for tungsten single crystals were calculated from first principles by means of the same methods as were used for Mo.[10] This means that the local-density approximation to the density-functional theory[11] was used together with the full-potential (FP) (Ref. 12) implementation of the linear muffin-tin orbital (LMTO) method[13] to calculate total energies of the crystal in various strain modes. We applied a scalar relativistic version of the LMTO scheme, i.e., relativistic shifts are correctly included, but spin-orbit splittings are omitted. Applying volume conserving strains in the [001] and [111] directions then allowed calculation of the tetragonal, $C'=\frac{1}{2}(C_{11}-C_{12})$, and trigonal, C_{44}, shear constants.

The FP-LMTO calculations were performed for volumes ranging from a 15% expansion down to 0.40 V_0, where V_0 is the experimental equilibrium volume corresponding to a lattice constant $a=3.165$ Å of the body-centered-cubic (bcc) unit cell. The calculations cover a large volume range, and this means that some states, which can be considered as being corelike for the zero-pressure volume, form rather broad bands at the strongly reduced volumes. For the sake of numerical continuity of the calculated energy versus volume relations, we used, at all volumes, the same grouping into ''core'' and ''valence'' electrons, and all calculations were performed in two energy ''panels.'' We considered 38 electrons as ''valence'' electrons, 18 of which (4*d*, 5*s*, 5*p*) were treated in the lower ''semicore'' panel, whereas 20 electrons occupied 4*f*-, 5*d*-, 6*s*-, and 6*p*-derived states in the upper energy range. The remaining electrons were considered as belonging to the core, but their wave functions were relaxed, i.e., recalculated in each iteration. Three sets of envelope functions were used (''triple-κ'' basis). Their formal kinetic energies were chosen to be -0.01, -1.0, and -2.3 Ry, respectively. The maximum angular momentum included in the basis were 3 (*spdf*), 3 (*spdf*), and 2 (*spd*) for the three tail kinetic energies, respectively. This means that 41 functions per atom were included.

Reciprocal-space integrations were performed by sampling special points for the lower panel contributions, whereas the tetrahedron method[14,15] was used in the upper panel. More than 1400 irreducible k points were required to obtain sufficient numerical accuracy in the total-energy variations.

The total energies were calculated for five tetragonal and

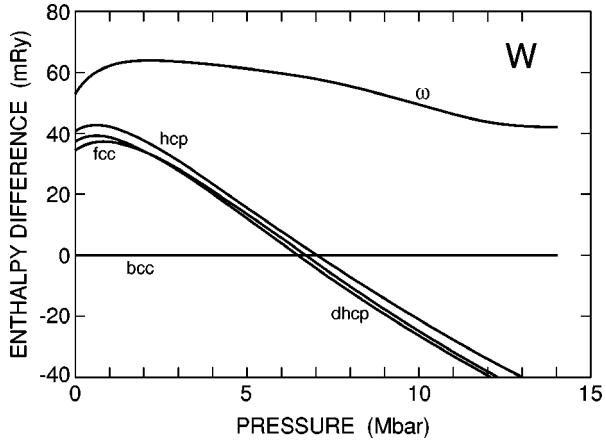

FIG. 1. Calculated enthalpies versus pressure of W in the ω phase, hcp, fcc, bcc, and dhcp phases. The bcc structure has been used as a reference.

five trigonal volume conserving distortions for each of 17 chosen volumes in the range mentioned earlier. Polynomial least-squares fits of the energy versus strain parameter were then used to derive the elastic constants as functions of volume. The theoretical pressure-volume (P-V) relation was obtained from the volume derivative of the energy-versus-volume (E-V) curve as obtained by fitting a suitable series to the energies obtained for the unsheared crystal. This also yielded the bulk modulus B as a function of volume.

III. CALCULATED PHASE STABILITY

The stability of the bcc phase of tungsten at high pressures was examined by comparing its theoretical total energy to those of other structures. The authors decided to consider the fcc, hpc, dhcp, and the ω titanium phases (see Ref. 16). From the calculated E-V and P-V relations we then derived the enthalpy for each of the phases versus pressure, as shown in Fig. 1. It is seen that the calculations predict that for $T=0$, the bcc structure is stable up to ≈ 6.5 Mbar, at least when comparison is made within this selection of structures. Figure 1 also suggests that the dhcp structure is energetically favored over the fcc at high pressures, but the enthalpy differences are so small that a definite order assignment cannot be made on the basis of these calculations. Thus, our calculations suggest that W undergoes a structural change from bcc to either fcc or dhcp when the applied pressure exceeds ≈ 6.5 Mbar.

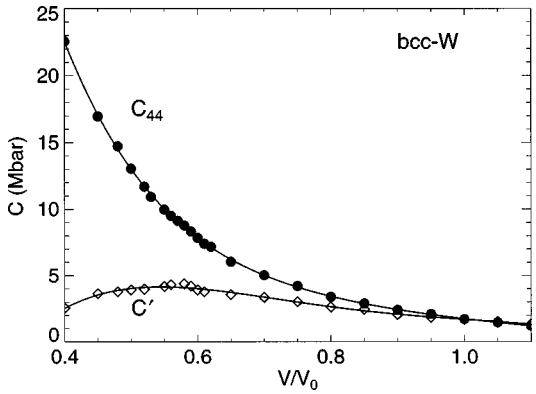

FIG. 2. The shear constants of bcc W as calculated as a function of volume. $C'=(C_{11}-C_{12})/2$.

TABLE I. Tungsten (bcc): Lattice constant, a (Å), relative volume, V/V_0, V_0 being the experimental equilibrium volume, pressure, P, bulk modulus, B,tetragonal, C', and trigonal, C_{44}, shear constants. P, B, C' and C_{44} are in units of Mbar. $[C'=\frac{1}{2}(C_{11}-C_{12})]$.

a	V/V_0	P	B	C'	C_{44}
3.165	1.00	-0.033	3.065	1.668	1.705
3.111	0.95	0.141	3.754	1.844	2.102
3.055	0.90	0.366	4.576	2.056	2.396
2.998	0.85	0.655	5.563	2.446	2.895
2.938	0.80	1.028	6.756	2.619	3.391
2.875	0.75	1.510	8.213	3.013	4.213
2.810	0.70	2.137	10.02	3.350	5.034
2.741	0.65	2.962	12.31	3.569	6.037
2.669	0.60	4.062	15.29	3.918	7.852
2.593	0.55	5.562	19.33	4.175	9.984
2.512	0.50	7.662	25.00	3.928	13.05
2.425	0.45	10.71	33.23	3.630	16.96
2.332	0.40	15.30	45.08	2.544	22.56

IV. ELASTIC CONSTANT RESULTS

Results of the calculations of pressure and elastic constants versus fractional volume are listed in Table I. The theoretical equilibrium volume is 0.9894 V_0, i.e., $\approx 1\%$ smaller than the experimental volume at $P=0$. The bulk modulus is 3.065 Mbar for $V=V_0$, close to the observed room-temperature value, 3.11 Mbar.[17]

Experimental values[18] at $V/V_0=1$ for C_{44} at $T=0$ K and 300 K are 1.631 and 1.607 Mbar, respectively, whereas Ref. 19 gives the values 1.627 at 77 K and 1.604 at 300 K. The measured C' values are 1.638 (0 K, Ref. 18), 1.594 (300 K, Ref. 18), 1.633 (77 K, Ref. 19), and 1.598 Mbar (300 K, Ref. 18). As follows from Table I, our calculated elastic constants, $C_{44}=1.705$ and $C'=1.668$ Mbar, are somewhat larger. The recent study of phonon instabilities in W, of Ref. 7, also included the calculation of the elastic constants.

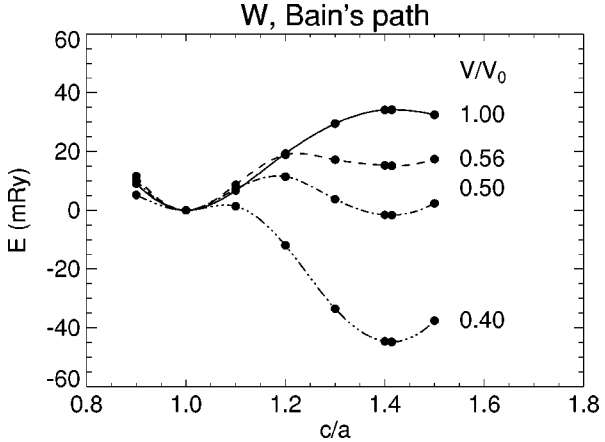

FIG. 3. Energy versus c/a ratio along Bain's transition path for various values of V/V_0.

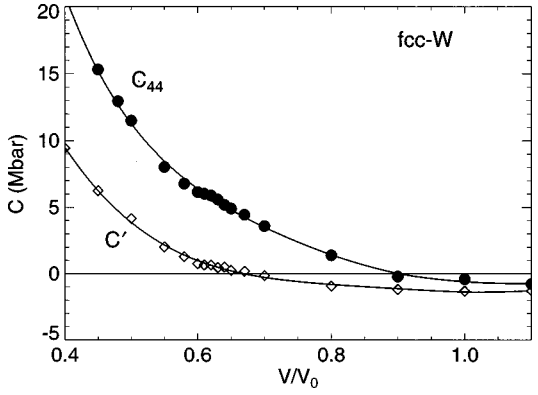

FIG. 4. The shear constants of the fcc structures of tungsten.

These norm-conserving pseudopotential calculations gave $C_{44}=1.49$ Mbar, $C'=1.74$ Mbar, and $B=3.2$ Mbar. Thus, C' of Ref. 7 is very close to our value whereas their C_{44} is considerably lower, and even below the measured values. We can also compare the pressure variations of the elastic constants as obtained in Ref. 7, and by us by evaluating the ratios $C(V/V_0)/C(1)$. We get $C'(0.656)/C'(1)=1.98$ and $C_{44}(0.656)/C_{44}(1)=3.58$, and the corresponding results of Ref. 7 are 1.54 and 3.30, respectively.

The pressure coefficients $\partial C_{44}/\partial P, \partial C'/\partial P$ and $\partial B/\partial P$ were measured by Katahara and co-workers[20] to be (at $P=0$): 1.609, 1.406, and 4.29, respectively. Our corresponding theoretical pressure coefficients are 1.99, 1.51, and 4.09, again illustrating that our C_{44} is overestimated. Comparing instead the pressure coefficients to those corresponding to relative changes, it is found that the experimental[20] values of $(C_{44})^{-1}\partial C_{44}/\partial P, (C')^{-1}\partial C'/\partial P$, and $B^{-1}\partial B/\partial P$, 1.00, 0.88, and 1.38 Mbar^{-1} are very close to those obtained in the present calculations; 1.08, 0.88, and 1.33 Mbar^{-1}.

The phase instability (preceding section) can also be seen in the constants. Whereas C_{44} increases with P, as illustrated in Fig. 2 (Table I as well), C' softens dramatically when V/V_0 is reduced below ≈ 0.55. This softening can be associated with an instability of the bcc structure to a tetragonal deformation that changes the structure to fcc along Bain's path (bcc is bct with $c/a=1$, fcc is bct with $c/a=\sqrt{2}$) (see Fig. 3). In Ref. 7 this instability was examined, including the pressure-induced anomalies in the phonon dispersion relations. Figure 4 shows the computed elastic constants of the possible high-pressure fcc structure of tungsten. Note that there is a macroscopic elastic instability for V/V_0 above ≈ 0.65.

V. EQUATION OF STATE

There is a comprehensive shock-based equation of state available for tungsten.[21] It is useful to compare this and the present theoretical results in a practical range of pressure. In experiments on hydrogen, at the highest pressure,[22] the lattice parameters ratio was $a/a_0=0.8625$ for the x-ray marker, tungsten. The 0 K pressures obtained for this ratio are shown in Table II. (The shock-based 300 K isotherm gives $P=327.4$ Mbar.) The theoretical data has been fitted to the two-parameter Birch equation[23] of state and to the two-parameter Vinet equation[24] to obtain the parameters called B_0 and B_0'. These are sensitive to the form of the equation used in the fit. The agreement of the four pressures is quite good, with a spread of 1%.

TABLE II. Experimental and theoretical values of B_0 and B_0' for W and of the pressure at $a/a_0=0.8625$ at $T=0$K.

EOS	B_0 (GPa)	B_0'	Ref.	P(GPa) for $a/a_0=0.8625$
Shock			20	327.4
(FP) LMTO (Birch)	326.8	3.685	20	324.7
(FP) LMTP (Vinet)	318.8	3.959	20	325.5
DFL-R (Birch)	320	3.80	7	328

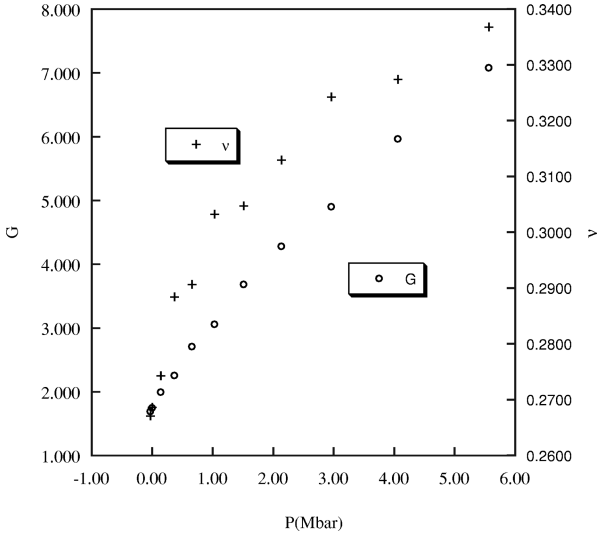

FIG. 5. The variation of the shear modulus G and the Poisson ratio ν of polycrystalline tungsten with pressure.

VI. MULTIMEGABAR RHEOLOGY

The plastic flow of materials at multimegabar pressures is of interest in the earth and other planets and in the diamond-anvil cell where the plastically flowing metal gasket contains the sample. The increase of the compressive yield stress with pressure, or pressure strengthening, has been considered in

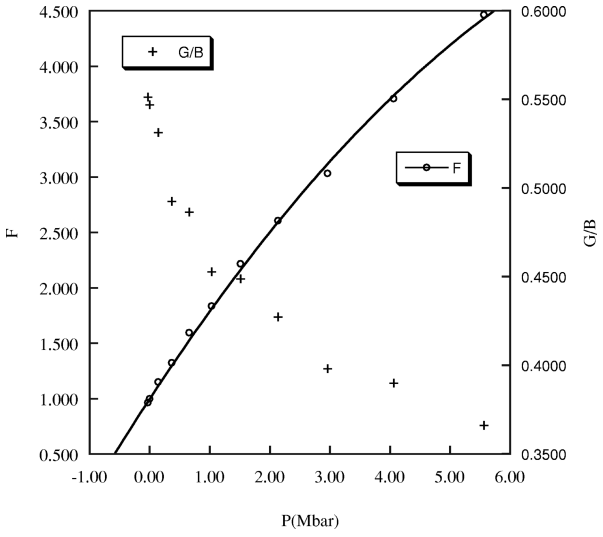

FIG. 6. The pressure strengthening factor F and the variation of G/B with pressure.

detail theoretically for molybdenum.[10] The containment of samples within gaskets of Mo, W, and Fe at multimegabar pressures is possible because of pressure strengthening. The variation of the yield strength of tungsten versus pressure has been studied experimentally using x-ray diffraction in the diamond-anvil cell.[25] An excellent historical description of the development of stress measurement (or elastic coefficient measurement) by x-ray diffraction is given in the book by Noyan and Cohen.[26] While the data of Ref. 25 show considerable scatter, it is possible that future studies will show improvement. It is therefore reasonable to examine the pressure strengthening of tungsten theoretically. Tungsten is also important because it was the gasket material in the first static experiment on H_2 to exceed 3 Mbar,[4] and appears not to react with H_2 at room pressure.

Chua and Ruoff[9] noted that for a polycrystalline aggregate that was elastically isotropic, the yield stress, if controlled by the motion of screw dislocations or by the motion of edge dislocations, scales with the shear modulus G or $G/(1-\nu)$, where ν is Poisson's ratio. High-pressure experimental studies favor the latter,[9] so for the yield stress at pressure, $\sigma_0(P)$,

$$\sigma_0(P)=[G(1-\nu_0)/G_0(1-\nu)]\sigma_{00}=F(P)\sigma_{00}. \quad (1)$$

Here, σ_{00} is the yield stress at zero pressure and $F(P)$ is the pressure-strengthening factor.

The upper and lower bounds of the shear modulus G of a randomly oriented aggregate can be calculated from the three elastic constants of the single crystal using the method of Hashin and Shtrikman,[8] and G itself can be assumed to be the average of these bounds. From G and the bulk modulus B, ν can be obtained. The variation of G and ν is shown in Fig. 5. In this way $F(P)$ is obtained as shown in Fig. 6. This function is well described by $F(P)=1+0.829P-0.0431P^2$ ($P\leqslant 6$ Mbar). When $F(P)\sigma_{00}$ is least-squares fitted to the experimental yield stress data for tungsten,[25] $\sigma_0(P)$, the value of σ_{00} that best fits the data is found to be $\sigma_{00}=4.9$ GPa. Direct measurement of the yield strength of the center region of a preindented gasket at atmospheric pressure would be very useful. This, together with much more accurate experimental measurements of $\sigma_0(P)$, would provide a direct comparison with the $F(P)$ computed here.

There have been many studies on the nature of the variation of the bulk modulus versus pressure. In particular, shock data gives extensive data on $B(P)$. Were G to have the same pressure dependence as B, then $G(P)$ could be obtained readily. This hypothesis is tested in Fig. 6. There is substantial variation of $G/B$with pressure, the value dropping over the range of available static pressures [560 GPa (Ref. 27)] by 33% in the present case. Of course G/B would not vary with pressure if ν did not vary with pressure (see Fig. 5).

VII. CONCLUSIONS

Theoretical calculations have progressed from the calculation of the bulk modulus and the equation of state to the calculation of single-crystal moduli as a function of pressure, and now to the calculation of rheological properties, such as the pressure dependence of the yield stress in the multimegabar range.

The equation of state computed here for W shows excellent agreement with the shock-based equation of state. Both C_{44} and B increase monotonically with pressure, while C' reaches a maximum in the neighborhood of the phase transition calculated at 6.5 Mbar and then decreases substantially with pressure (if the bcc phase is assumed to persist). The shear elastic constants of the high-pressure fcc phase are negative at low pressure but become positive at higher pressures and continue to increase with pressure at high pressures. The energy barrier for the Bain transition path from bcc to fcc W was computed. The elastic moduli of a randomly oriented polycrystalline aggregate of tungsten was computed from the single-crystal moduli. This was used to compute the pressure dependence of the yield strength that is required for calculating the plastic behavior of the gasket in the anvil cell. It is the large pressure-strengthening factor (4.5 at 6 Mbar) that makes possible the attainment of multimegabar pressures in the diamond-anvil cell.

ACKNOWLEDGMENT

We acknowledge support by the National Science Foundation Grant No. DMR-9530634.

[1] A. L. Ruoff, in *High Pressure Science and Technology*, edited by W. A. Trzeciakowski (World Scientific, New Jersey, 1996), p. 511.
[2] Y. K. Vohra, S. J. Duclos, and A. L. Ruoff, Phys. Rev. B **36**, 9790 (1987).
[3] A. L. Ruoff, H. Xia, H. Luo, and Y. K. Vohra, Rev. Sci. Instrum. **61**, 3830 (1990).
[4] C. Narayana, J. Orloff, and A. L. Ruoff, Rev. High Pressure Sci. Technol. **7**, 772 (1998).
[5] D. A. Young, *Phase Diagrams of the Elements* (University of California, Los Angeles, 1991).
[6] N. E. Christensen, A. L. Ruoff, and C. O. Rodriguez, Phys. Rev. B **52**, 9121 (1995).
[7] K. Einarsdotter, B. Sadigh, G. Grimvall, and V. Ozolins, Phys. Rev. Lett. **79**, 2073 (1997).
[8] Z. Hashin and S. Shtrikman, J. Mech. Phys. Solids **10**, 343 (1962).
[9] J. O. Chua and A. L. Ruoff, J. Appl. Phys. **46**, 4659 (1975).
[10] N. E. Christensen, A. L. Ruoff, and C. O. Rodriguez, Phys. Rev. B **52**, 9121 (1995).
[11] P. Hohenberg and W. Kohn, Phys. Rev. **136**, B864 (1964); W. Kohn and L. J. Sham, *ibid.* **140**, A1133 (1965); L. J. Sham and W. Kohn, *ibid.* **145**, 561 (1966); the present calculations used the parametrization of Barth-Hedin, U. von Barth, and L. Hedin, J. Phys. C **5**, 1629 (1972).
[12] M. Methfessel, Phys. Rev. B **38**, 1537 (1988); M. Methfessel, C. O. Rodriguez, and O. K. Andersen, *ibid.* **40**, 2009 (1989).
[13] O. K. Andersen, Phys. Rev. B **12**, 3060 (1975).
[14] O. Jepsen and O. K. Andersen, Phys. Rev. B **29**, 5965 (1984).

[15] P. Blöchl, O. Jepsen, and O. K. Andersen, Phys. Rev. B **49**, 16 223 (1994).
[16] K.-M. Ho, C.-L. Fu, and B. N. Harmon, Phys. Rev. B **29**, 1575 (1984).
[17] G. Bradfield, as referenced in G. W. C. Kaye and T. H. Laby, *Tables of Physical and Chemical Constants*, 13th ed. (Longmans, Green & Co. Ltd., London, 1966).
[18] F. H. Featherston and J. R. Neighbors, Phys. Rev. **130**, 1324 (1963).
[19] D. I. Bolef and J. de Klerk, J. Appl. Phys. **33**, 2311 (1962).
[20] K. W. Katahara, M. H. Manghnani, and E. S. Fisher, J. Phys. F **9**, 733 (1979).
[21] R. S. Hixson and J. N. Fritz, J. Appl. Phys. **71**, 1721 (1992).
[22] C. Narayana, H. Luo, J. Orloff, and A. L. Ruoff, Nature (London) **393**, 46 (1988).
[23] F. Birch, J. Geophys. Res. **83**, 1257 (1978).
[24] P. Vinet, J. Ferrante, J. R. Smith, and J. H. Rose, J. Phys. C **19**, 467 (1986).
[25] T. J. Hemley, H-k. Mao, G. Shen, J. Badro, P. Gillet, M. Hanfland, and D. Häusermann, Science **276**, 1242 (1997).
[26] I. C. Noyan and J. B. Cohen, *Residual Stress Measurement by Diffraction and Interpretation* (Springer-Verlag, New York, 1987).
[27] A. L. Ruoff, H. Xia, and Q. Xia, Rev. Sci. Instrum. **63**, 4342 (1992).